

theoretical value of  $10^4 U$  would then be 1.04, instead of the entry 1.19 in Table VI.

Electrophoretic titrations provide interesting examples of the possibilities. Suppose that a fully neutralized poly(weak acid), such as the one used by Meulenet et al.,<sup>27</sup> is titrated with protons. If the metal counterions are territorially bound, then, since all of the protons are site-bound, the appropriate value of  $b$  is  $b_1 \alpha^{-1}$ , where  $b_1$  is the structural charge spacing at full neutralization ( $\alpha = 1$ ). This procedure is the basis of the theoretical correlation of the data in Table VII, where  $U_{\text{theory}}$  is an increasing function of  $\alpha$ . In principle, a similar case should arise when a polyphosphate salt with univalent counterions is titrated by  $\text{Mg}^{2+}$ , since the latter is presumably site-bound to polyphosphate, at least in the initial titration stage.<sup>10,36</sup> The prediction, then, is that  $U$  decreases as  $\text{Mg}^{2+}$  is added. Available data are puzzling,<sup>37</sup> as the prediction appears to be correct if the univalent counterion is  $(\text{CH}_3)_4\text{N}^+$ , while, for  $\text{Na}^+$ , initial titration with  $\text{Mg}^{2+}$  does not modify  $U$  (see Figure 4 of ref 37). A problem in the interpretation may be the high concentration of 1:1 salt in the solutions. As noted above in connection with the data of Strauss et al.<sup>25,26</sup> (Table VI), the observed value of  $U$  in 0.2 M  $(\text{CH}_3)_4\text{N}^+$  is much higher than in the same concentration of  $\text{Na}^+$ , contrary to prediction. However, at 0.01 M 1:1 salt, the situation is "normal", the corre-

sponding mobilities being almost the same (see above). It would thus be of interest to have  $\text{Mg}^{2+}$  titration data at lower salt concentrations.

Consider next a case for which both the univalent cation and the titrating divalent metal cation are territorially bound, a situation that probably arises in DNA solutions, for example.<sup>2</sup> The value of  $b$  for the model remains fixed at the structural value throughout the titration. The initial version of counterion condensation theory for mixed uni-divalent counterion systems<sup>38</sup> would predict an initially invariant polyion charge with consequent invariance of the mobility, but the predictions of current theory<sup>2</sup> are more complex. Figure 5 of ref 2 shows that the net polyion charge decreases monotonically as more divalent cations are territorially bound; invariant-charge behavior is the limiting envelope as the ionic strength tends to zero. Therefore the prediction again is that  $U$  decreases as titration proceeds, a qualitative behavior which has been observed,<sup>39</sup> although the data are perhaps not clear-cut, the  $(\text{CH}_3)_4\text{N}^+$  univalent cation employed having since been found to interact specifically with DNA.<sup>22,23</sup>

It is conceivable that territorially bound and site-bound titrating ions may be distinguished on a quantitative level by the distinct theoretical calculations employed to model them.

(36) P. Spegt and G. Weill, *Biophys. Chem.*, **4**, 143 (1976).

(37) U. P. Strauss and A. Siegel, *J. Phys. Chem.*, **67**, 2683 (1963).

(38) G. S. Manning in "Polyelectrolytes", E. Sélégny, Ed., Reidel, Dordrecht, Holland, 1974.

(39) P. D. Ross and R. L. Scruggs, *Biopolymers*, **2**, 79 (1964).

## Crossed Molecular Beam Studies of Proton Transfer, Unimolecular Decay, and Isotope Scrambling in the Reactions $\text{H}_2^+ + \text{H}_2\text{O}$ , $\text{H}_2^+ + \text{D}_2\text{O}$ , and $\text{D}_2^+ + \text{H}_2\text{O}$

R. M. Bilotta and J. M. Farrar\*

Department of Chemistry, University of Rochester, Rochester, New York 14627 (Received: December 1, 1980)

We present an experimental study of the title reactions over the collision energy range from 0.7 to 6.9 eV. Over the entire collision energy range, a significant fraction of the products have internal excitation sufficiently high to undergo unimolecular decay to  $\text{H}_2\text{O}^+$  or an isotopically substituted water cation. An examination of the reactions  $\text{D}_2^+ + \text{H}_2\text{O}$  and  $\text{H}_2^+ + \text{D}_2\text{O}$  and observation of  $\text{H}_2\text{O}^+$  and  $\text{HOD}^+$  products of unimolecular decay at 3.0 and 6.3 eV suggest that, at the lower collision energy, the recoil energy distributions are consistent with the results of phase space calculations including all vibrations of the  $\text{H}_2\text{O}^+$  or  $\text{HOD}^+$  product. At this collision energy, the unimolecular decay products have barycentric angular distributions with sharp forward-backward symmetry, suggesting that planar scattering with concomitant angular momentum polarization is an important dynamical feature in these reactions. At the higher collision energy, the complex "osculates" with a lifetime too short for rapid intramolecular energy transfer. We also present evidence for a direct reaction between  $\text{H}_2^+$  and  $\text{D}_2\text{O}$  yielding  $\text{HOD}^+$  and a bound HD molecule, proceeding through a four-center exchange reaction rather than through unimolecular decay of  $\text{HD}_2\text{O}^+$ .

### Introduction

The study of ion-neutral reaction dynamics in the gas phase has experienced significant growth in recent years through the impetus of experimental and theoretical advances allowing ionic systems to be studied in increasing detail.<sup>1</sup> One of the ultimate goals of these studies is the elucidation of the dynamics of ion-neutral interactions in the single collision regime. The development of instru-

mentation for studying such interactions at low collision energies as well as theoretical techniques for computing potential surfaces and the dynamics of systems on these surfaces has begun to make this goal a realizable one.

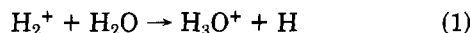
Within the broad category of ion-neutral interactions, proton transfer reactions are of special interest because of their intrinsic chemical simplicity and their pervasiveness in a wide variety of processes.<sup>2</sup> The realization that

(1) See, for example, M. T. Bowers, Ed., *Gas Phase Ion Chem.*, **1**, 2 (1979).

(2) R. W. Taft in "Kinetics of Ion-Molecule Reactions", P. Ausloos, Ed., Plenum Press, New York, 1979, p 271.

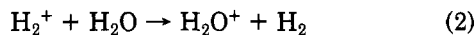
gas-phase ionic processes in general, and proton transfer reactions in particular, are of great importance in hydrocarbon flames<sup>3,4</sup> has generated new interest in ion-neutral interactions. The high proton affinity of water<sup>5</sup> makes the hydronium ion,  $\text{H}_3\text{O}^+$ , an extremely important constituent in a variety of systems including electrical discharges, combustion systems, and aqueous solutions. The  $\text{H}_3\text{O}^+$  ion has been identified as the primary ion in hydrocarbon flames,<sup>6</sup> with proton transfer from the formyl cation,  $\text{HCO}^+$ , to  $\text{H}_2\text{O}$  the accepted mechanism for its formation.<sup>6</sup> A study of proton transfer from a variety of acids to  $\text{H}_2\text{O}$  should be of value in systematizing and elucidating the chemical dynamics of  $\text{H}_3\text{O}^+$  formation in the gas phase.

In previous work from our laboratory, we have presented data on the proton transfer and charge transfer reactions of the simplest molecular ion,  $\text{H}_2^+$ , with  $\text{CO}^{7,8}$  and  $\text{Ar}$ ,<sup>9-11</sup> using the crossed molecular beam technique at low collision energies to measure angular and kinetic energy distributions of reaction products. One of the central motivations for such studies has been to examine the collision dynamics of systems which are sufficiently simple to allow fruitful comparison with theory. As part of a continuing program of study on the reactions of  $\text{H}_2^+$  with atoms and small molecules, we have initiated a study of the proton transfer reaction in eq 1 over the relative kinetic energy range

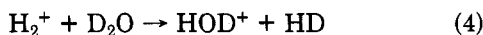
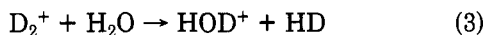


0.7–6.9 eV. This reactive system is sufficiently simple to be tractable theoretically, yet serves as a prototype for understanding the complexities of chemical reactions operative in systems of practical importance.

Of additional interest in the  $\text{H}_2^+ + \text{H}_2\text{O}$  system is the fact that the large exothermicity of 4.6 eV for reaction 1 makes unimolecular dissociation of the  $\text{H}_3\text{O}^+$  product an important channel at relatively low collision energies. The charge transfer process in eq 2 also competes with proton

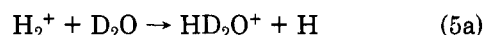


transfer and provides a channel for  $\text{H}_2\text{O}^+$  production in addition to unimolecular dissociation of  $\text{H}_3\text{O}^+$ , particularly at high collision energies. The charge transfer reaction 2 as written implies that electron transfer alone is responsible for  $\text{H}_2\text{O}^+$  formation, but the use of isotopically labeled reactants allows for the observation of atom transfer with simultaneous electron transfer, as indicated for reactions 3 and 4. The possibility that the neutral fragment HD



may also be unbound is a consequence of the unimolecular dissociation of the initially formed hydronium ion, exem-

plified in reaction sequence 5a and 5b. A study of the



kinematics and the energy dependence of the formation of  $\text{HOD}^+$  produced in reactions 4 and 5b can be used to distinguish between these competitive channels.

The  $\text{H}_2^+ + \text{H}_2\text{O}$  and  $\text{D}_2^+ + \text{H}_2\text{O}$  systems have been studied by Kim and Huntress<sup>12</sup> in thermal energy ICR experiments. In contrast with other molecules for which reaction with  $\text{H}_2^+$  leads exclusively to charge transfer,  $\text{H}_2\text{O}$  is unique because the proton transfer reaction at thermal energy has a rate constant nearly as large as that for charge transfer. The  $\text{D}_2^+ + \text{H}_2\text{O}$  system is particularly interesting in that  $\text{HOD}^+$  product is observed at thermal energies, where the vast majority of collisions are below threshold for unimolecular dissociation of  $\text{DH}_2\text{O}^+$ . The "wings" in the ICR line suggest that the  $\text{HOD}^+$  results from a process whose cross section increases with relative energy, in contrast to the line shape expected for an exothermic reaction exhibiting an  $E^{-1/2}$  energy dependence.

The present work reports on low-energy crossed beam studies of reactions 1–5 over an extended energy range, with the goal of elucidating the dynamics of proton transfer, isotope exchange, and unimolecular decay of "superexcited"  $\text{H}_3\text{O}^+$ . This range of collision energies is sufficiently small that electronically excited  $\text{H}_3\text{O}^+$ , predicted theoretically by Kaufman et al.<sup>13</sup> and observed experimentally by Koski and co-workers<sup>14</sup> ~12 eV above the ground state, is inaccessible. We also attempted to observe  $\text{H}_3^+$  in the reaction  $\text{H}_2^+ + \text{H}_2\text{O} \rightarrow \text{H}_3^+ + \text{OH}$  but did not see this product; nor did we see  $\text{D}_2\text{HO}^+$  from the reaction  $\text{D}_2^+ + \text{H}_2\text{O} \rightarrow \text{D}_2\text{HO}^+ + \text{H}$ .

## Experimental Section

The crossed beam apparatus used in these studies has been described in detail in previous work from our laboratory.<sup>8,9</sup> Ions produced by electron impact on  $\text{H}_2$ , and possessing a distribution of vibrational states given by Franck–Condon factors for vertical ionization of  $\text{H}_2$  ( $\nu = 0$ ), intersect a seeded supersonic beam of  $\text{H}_2\text{O}$  at  $90^\circ$  in a vacuum chamber maintained at  $2 \times 10^{-7}$ – $3 \times 10^{-7}$  torr by a cryogenically trapped oil diffusion pump. The distribution of vibrational states of  $\text{H}_2^+$  extends to  $\nu = 18$ , near the dissociation limit of ~2.7 eV. The distribution peaks at  $\nu = 2$  and has a mean of 0.89 eV, corresponding very closely to  $\nu = 3$ . The fwhm of the vibrational distribution is 1.2 eV.<sup>15</sup> The ion beam, whose laboratory energy varies from 0.7 to 7.6 eV and whose energy spread is 0.3 eV fwhm, intersects a neutral beam prepared by bubbling a carrier gas, usually  $\text{H}_2$ , at a pressure of 500 torr through liquid  $\text{H}_2\text{O}$  or  $\text{D}_2\text{O}$  at ~20 °C (partial pressure, 18 torr). The gas-handling lines are heated to avoid condensation. The seeding conditions employed yield a beam of  $\text{H}_2\text{O}$  whose most probable speed is  $2.24 \times 10^5$  cm s<sup>-1</sup>; although we have not measured the velocity distribution of the seeded  $\text{H}_2\text{O}$  beam, beams produced by similar techniques generally have Mach numbers exceeding 10, with fwhm velocity distributions of ~12–15%.<sup>16</sup> The neutral beam is modulated at 150 Hz by a tuning-fork chopper.

(12) J. K. Kim and W. T. Huntress, Jr., *J. Chem. Phys.*, **62**, 2820 (1975).

(13) R. C. Raffanetti, H. J. T. Preston, and J. J. Kaufman, *Chem. Phys. Lett.*, **46**, 513 (1977).

(14) R. J. Cotter and W. S. Koski, *J. Chem. Phys.*, **59**, 784 (1973).

(15) D. Villarejo, *J. Chem. Phys.*, **48**, 4014 (1968).

(16) J. J. Valentini, M. J. Coggiola, and Y. T. Lee, *Rev. Sci. Instrum.*, **48**, 58 (1977).

(3) D. K. Bohme in "Kinetics of Ion–Molecule Reactions", P. Ausloos, Ed., Plenum Press, New York, 1979, p 323.

(4) D. K. Bohme, J. M. Goodings, and C. W. Ng, *Int. J. Mass Spectrom. Ion Phys.*, **24**, 335 (1977).

(5) A compilation of proton affinities appears in R. Walder and J. L. Franklin, *Int. J. Mass Spectrom. Ion Phys.*, **36**, 85 (1980).

(6) J. A. Green and T. M. Sugden, *Symp. (Int.) Combust. [Proc.]*, **9**, 607 (1963).

(7) F. N. Preuninger, R. M. Bilotta, and J. M. Farrar, *J. Chem. Phys.*, **71**, 4166 (1979).

(8) R. M. Bilotta, F. N. Preuninger, and J. M. Farrar, *J. Chem. Phys.*, **72**, 1583 (1980).

(9) R. M. Bilotta, F. N. Preuninger, and J. M. Farrar, *J. Chem. Phys.*, **73**, 1637 (1980).

(10) R. M. Bilotta, F. N. Preuninger, and J. M. Farrar, *Chem. Phys. Lett.*, **74**, 95 (1980).

(11) R. M. Bilotta and J. M. Farrar, *J. Chem. Phys.*, **74**, 1699 (1981).

Defining the average value of the total energy as

$$\bar{E}_{\text{total}} = \bar{E}_{\text{T}} + \bar{E}_{\text{int}} - \Delta E_0^\circ$$

with  $\bar{E}_{\text{int}}$  defined as the average internal excitation of  $\text{H}_2^+$  comprising 0.89 eV of vibrational energy and 0.03 eV of rotational energy and  $\Delta E_0^\circ$  the reaction exothermicity, we compute the fractional spread in the total energy as

$$\Delta E_{\text{total}}/\bar{E}_{\text{total}} = (\Delta E_{\text{int}}^2 + \Delta E_{\text{T}}^2)^{1/2}/\bar{E}_{\text{total}}$$

$\Delta E_{\text{int}}$  and  $\Delta E_{\text{T}}$  are the fwhm values for the internal energy and initial translational energy distributions with values of 1.2 and 0.3 eV, respectively, yielding  $\Delta E_{\text{total}} = 1.24$  eV. The fractional spread in the total energy ranges from 0.20 at the lowest kinetic energy of 0.7 eV to 0.10 at the highest energy studied in these experiments, 6.9 eV.

Reactively scattered products are detected in the plane of the beams, in synchronization with the neutral beam modulation, by an energy analyzer–quadrupole mass spectrometer detector under control of a minicomputer–multichannel scaler. Data accumulated by the laboratory minicomputer are transferred to a campus mainframe computer for reduction and analysis as indicated later in this paper.

Normalization of the product translational energy scans at various laboratory angles is accomplished by measuring laboratory angular distributions, which effectively integrate over product laboratory energy at a given laboratory angle. The angular distributions are obtained by operating the detector in its usual energy scanning mode, but, rather than data being collected at various lab energies with a multichannel scaler, the signal is collected by a two channel scaler gated synchronously with the modulation of the neutral beam. In this manner, one scaler collects signal plus background counts, corresponding to the open period of the tuning-fork chopper, while the second scaler records background counts acquired during the closed period of the chopper.

### Reaction Thermodynamics

The tabulated proton affinities<sup>5</sup> of the hydrogen atom and of  $\text{H}_2\text{O}$  provide an estimate for the exothermicity of the proton transfer reaction 1 of 4.6 eV. The proton affinity of  $\text{H}_2\text{O}$  and the ionization potentials of the hydrogen atom and  $\text{H}_2\text{O}$  provide estimates for the energetics of the dissociation reactions of  $\text{H}_3\text{O}^+$  as indicated by eq 6 and 7.<sup>17</sup>



Because of kinematic constraints and the inherent difficulty of proton detection with a quadrupole mass spectrometer, we may expect to observe only the  $\text{H}_2\text{O}^+$  product of  $\text{H}_3\text{O}^+$  unimolecular decomposition. Energy conservation in conjunction with the  $\text{H}_2^+$  internal excitation indicates that  $\text{H}_3\text{O}^+$  products formed at relative collision energies greater than or equal to  $\sim 0.7$  eV will have sufficient internal energy to dissociate via formation of  $\text{H}_2\text{O}^+$ . Thus, unimolecular decomposition of  $\text{H}_3\text{O}^+$  plays a role in the proton transfer dynamics over the entire energy range of these experiments.

A comparison of the ionization potentials for  $\text{H}_2$  and  $\text{H}_2\text{O}$  indicates that the charge transfer reaction 2 is exothermic by 2.8 eV, and, therefore, neglecting small zero-point energy differences of significantly less than 0.1 eV, the simultaneous charge transfer–atom transfer reactions 3 and 4 are also exothermic by  $\sim 2.8$  eV.

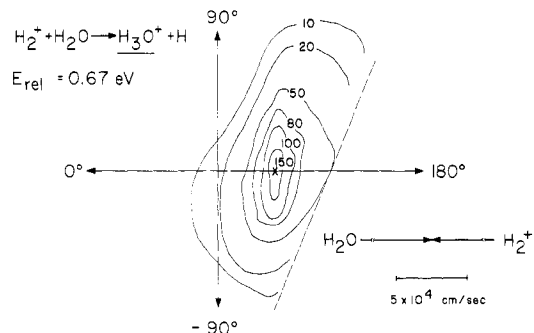


Figure 1. Barycentric polar flux contour map for  $\text{H}_2^+ (\text{H}_2\text{O}, \text{H})\text{H}_3\text{O}^+$  at 0.67 eV. Spectator stripping point marked by X.

### Data Analysis

Data collection consists of measuring arrays of laboratory energy fluxes at selected laboratory scattering angles. A typical experiment at a single collision energy consists of collecting product energy fluxes with a 50-channel multiscaler at 10–30 laboratory angles. Barycentric polar flux distributions are extracted from the laboratory data by iterative deconvolution of the dispersion in initial reactant velocities and beam intersection angles. The deconvolution procedure, a modification of a technique developed by Siska,<sup>18</sup> solves the equation

$$I_{\text{lab}}(v, \theta) = \sum_i h_i (v^2/u_i^2) I_{\text{cm}}(u_i, \theta_i)$$

iteratively for  $I_{\text{cm}}(u_i, \theta_i)$ , where the variables  $v$  and  $\theta$  are laboratory coordinates and  $u_i$  and  $\theta_i$  are barycentric coordinates.

The summation extends over a grid of Newton diagrams describing the initial beam velocity dispersions, the probability of the  $i$ th Newton diagram denoted by  $h_i$ . The nonseparable barycentric polar flux  $I(u, \theta)$  may be presented as a contour map in polar coordinates. In order to assess energy disposal and product angular distributions, the barycentric polar flux may also be averaged appropriately to yield angle averaged translational energy distributions and recoil speed averaged angular distributions through the following relations:

$$P(E_{\text{T}}') = \sum_i I_{\text{cm}}(E_{\text{T}}', \theta_i) \sin \theta_i \\ = \sum_i u_i^{-1} I_{\text{cm}}(u_i, \theta_i) \sin \theta_i$$

$$P(f_{\text{T}}') = \bar{E}_{\text{total}} \sum_i I_{\text{cm}}(E_{\text{T}}', \theta_i) \sin \theta_i$$

$$g(\theta) = \sum_i I(u_i, \theta)$$

where  $f_{\text{T}}' = E_{\text{T}}'/\bar{E}_{\text{total}}$ ,  $E_{\text{T}}'$  being the product translational energy. The deconvolution procedure yields barycentric cross sections which, when transformed to the laboratory coordinate system with appropriate averaging over the experimental conditions, recover the experimental data with a standard deviation between 3% and 7%.

### Results

The proton transfer reaction 1 has been studied at seven different relative energies ranging from 0.7 to 6.9 eV. The global properties of the scattering can be assessed by considering polar flux contour maps in the barycentric system; such maps for three of the energies of these experiments are shown in Figures 1–3. The maps demonstrate immediately that the proton transfer reaction is a direct process, in which  $\text{H}_2\text{O}$  removes a proton from  $\text{H}_2^+$

(17) H. M. Rosenstock et al., *J. Phys. Chem. Ref. Data, Suppl.*, 1 6, (1977).

(18) P. E. Siska, *J. Chem. Phys.*, 59, 6052 (1973).

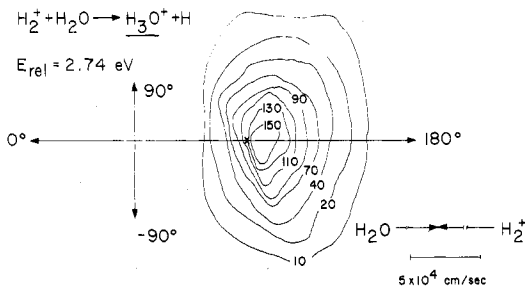


**Figure 2.** Barycentric polar flux contour map for  $\text{H}_2^+(\text{H}_2\text{O},\text{H})\text{H}_3\text{O}^+$  at 2.74 eV. Spectator stripping point marked by X.

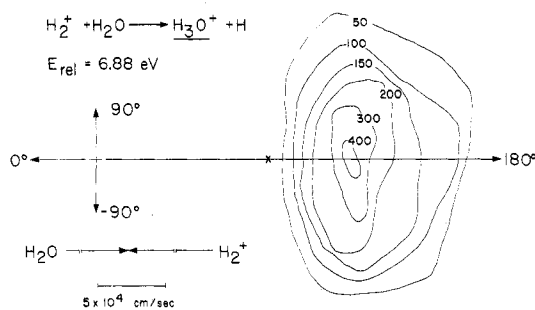


**Figure 3.** Barycentric polar flux contour map for  $\text{H}_2^+(\text{H}_2\text{O},\text{H})\text{H}_3\text{O}^+$  at 6.88 eV. Spectator stripping marked by X.

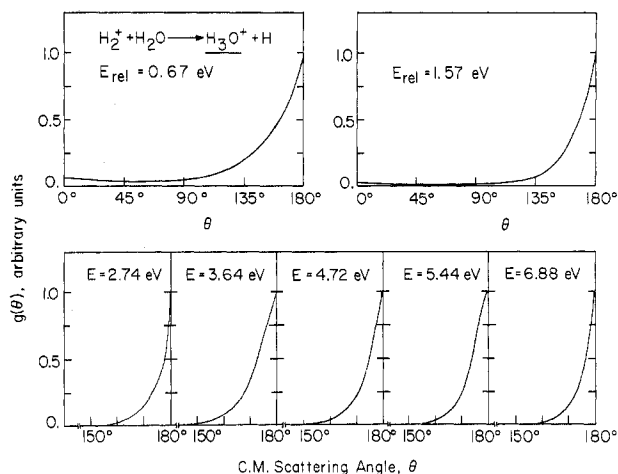


**Figure 4.** Barycentric angular distributions extracted by deconvolution for  $\text{H}_2^+(\text{H}_2\text{O},\text{H})\text{H}_3\text{O}^+$  at relative energies between 0.67 and 6.88 eV.

in a "stripping"-type encounter with very little momentum transfer between products.<sup>19,20</sup> Figure 4 shows  $\text{H}_3\text{O}^+$  product angular distributions extracted from the experimental data using the deconvolution procedure described above. The angular distributions are all peaked at  $\theta = \pi$ , consistent with the direct interaction noted in the contour maps. The angular distributions are all quite narrow, with a slight tendency to broaden as the collision energy is reduced from 6.9 to 0.7 eV. The direct nature of the reaction is consistent with the fact that experimental<sup>21,22</sup> work on the related system  $\text{H}_3\text{O}^+ + \text{H}_2 \rightarrow \text{H}_3\text{O}^+ + \text{H}$  shows no evidence for a long-lived  $\text{H}_4\text{O}^+$  intermediate.

Figure 5 shows product recoil energy distributions plotted as a function of  $f_T' = E_T'/\bar{E}_{\text{total}}$ , where  $E_T'$  is the

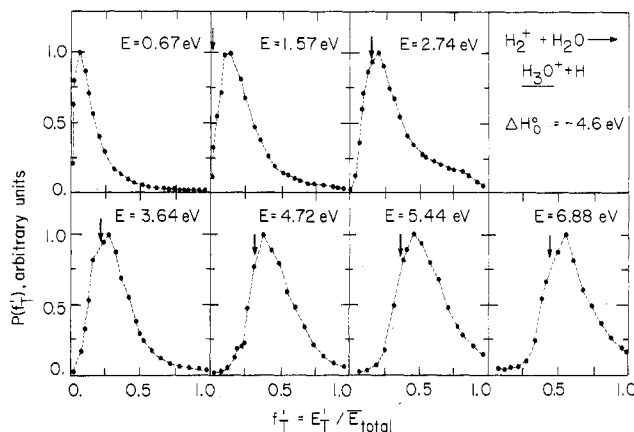


**Figure 5.** Barycentric recoil energy distributions  $P(f_T')$  for  $\text{H}_2^+(\text{H}_2\text{O},\text{H})\text{H}_3\text{O}^+$  at relative energies between 0.67 and 6.88 eV. Arrows denote minimum translational energy below which  $\text{H}_3\text{O}^+$  is unstable with respect to  $\text{H}_2\text{O}^+ + \text{H}$ .

product translational energy and  $\bar{E}_{\text{total}}$  is the average value of the total energy available to the system. Because of the possibility that  $\text{H}_3\text{O}^+$  may dissociate via reactions 6 and 7, there exists a minimum value of  $f_T'$  at each collision energy below which  $\text{H}_3\text{O}^+$  products are unstable with respect to these dissociative channels. A lower limit on the minimum translational energy which stable  $\text{H}_3\text{O}^+$  products may have is given by the following expression:

$$E_T'(\text{min}) = E_r + \bar{E}_T - \Delta E_0^\circ - E_{\text{threshold}}$$

where  $E_r$  is the rotational energy of the  $\text{H}_2^+$  reagent,  $\bar{E}_T$  is the initial relative translational energy,  $\Delta E_0^\circ$  is the reaction exothermicity, and  $E_{\text{threshold}}$  is the threshold energy for dissociation of  $\text{H}_3\text{O}^+$  to  $\text{H}_2\text{O}^+$ , given as 6.2 eV. The corresponding value of  $f_T'(\text{min})$  may be defined as  $E_T'(\text{min})/\bar{E}_{\text{total}}$ . The  $P(f_T')$  distributions of Figure 5 are marked with arrows at the appropriate values of  $f_T'(\text{min})$  below which products are unstable to dissociation.<sup>23</sup> The appearance of product below  $f_T'(\text{min})$  is a reflection of the finite energy and angular resolution of our apparatus.

The effects of product dissociation are portrayed very clearly in the  $P(f_T')$  distributions, showing depletion at low values of  $f_T'$ , the most probable values of  $f_T'$  always falling slightly above the minimum allowed values of  $f_T'$ . The proton transfer reaction thus appeared to channel sufficient energy into the products to yield  $\text{H}_3\text{O}^+$  which is maximally excited, subject to the constraints of product stability. This situation contrasts markedly with our results on  $\text{H}_2^+ + \text{Ar}$ , in which  $\text{HAr}^+$  products are observed in the "forbidden" region at low  $f_T'$ , the extent of superexcited product formation increasing with relative collision energy.<sup>9</sup>

The depletion of the  $P(f_T')$  distributions at low  $f_T'$  provides striking evidence for product dissociation via channels 6 and 7. The reaction  $\text{H}_2^+ + \text{H}_2\text{O} \rightarrow \text{H}^+ + \text{H} + \text{H}_2\text{O}$  could proceed via direct collision-induced dissociation (CID)<sup>25</sup> of  $\text{H}_2^+$  as written, or sequentially, in which  $\text{H}_3\text{O}^+$  produced by proton transfer from  $\text{H}_2^+$  to  $\text{H}_2\text{O}$  undergoes unimolecular decay<sup>24</sup> to the products indicated; these channels are experimentally indistinguishable. The reaction  $\text{H}_2^+ + \text{H}_2\text{O} \rightarrow \text{H}_2\text{O}^+ + \text{H} + \text{H}$  may proceed in a single dissociative charge transfer step as written, or by unimolecular decay of nascent  $\text{H}_3\text{O}^+$ . We will present data later which support the latter possibility.

(19) A. Henglein, K. Lacmann, and G. Jacobs, *Ber. Bunsenges. Phys. Chem.*, **69**, 279 (1965).

(20) D. R. Herschbach, *Appl. Opt.*, **Suppl. 2**, 128 (1965).

(21) A. J. Yencha, V. Pacák, and Z. Herman, *Int. J. Mass Spectrom. Ion Phys.*, **26**, 205 (1978).

(22) C. A. Jones, K. L. Wendell, and W. S. Koski, *J. Chem. Phys.*, **63**, 2254 (1975).

(23) T. M. Mayer, B. E. Wilcomb, and R. B. Bernstein, *J. Chem. Phys.*, **67**, 3507 (1977).

(24) R. A. LaBudde, P. J. Kuntz, R. B. Bernstein, and R. D. Levine, *J. Chem. Phys.*, **59**, 6286 (1973).

(25) R. D. Levine and R. B. Bernstein, *Chem. Phys. Lett.*, **11**, 552 (1971).

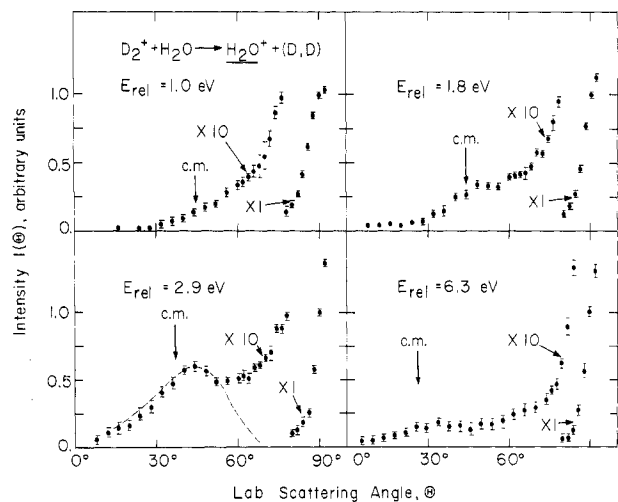


**Figure 6.** Laboratory angular distributions for  $\text{H}_2\text{O}^+$  produced in collisions of  $\text{D}_2^+$  with  $\text{H}_2\text{O}$  at collision energies indicated. Dotted curve in 2.9-eV experiment is the fit resulting from deconvolution of energy scans of  $\text{H}_2\text{O}^+$  produced by unimolecular decay of  $\text{DH}_2\text{O}^+$ .

A more direct probe of  $\text{H}_3\text{O}^+$  product decay than that afforded by observing depletion in the  $P(f_T)$  distributions can be achieved by direct detection of such  $\text{H}_2\text{O}^+$  products. We have performed a number of experiments with isotopically labeled reagents with the goal of detecting the products of unimolecular decay directly.<sup>26,27</sup> In particular, we have considered collisions of  $\text{D}_2^+$  with  $\text{H}_2\text{O}$ , and  $\text{H}_2^+$  with  $\text{D}_2\text{O}$ , in which the products of deuteron and proton transfer are  $\text{DH}_2\text{O}^+$  and  $\text{HD}_2\text{O}^+$ , respectively. When the available energy exceeds the dissociation threshold, these ions can eject either H or D atoms; thus  $\text{DH}_2\text{O}^+$  may yield  $\text{HOD}^+$  or  $\text{H}_2\text{O}^+$ , and  $\text{HD}_2\text{O}^+$  will yield  $\text{HOD}^+$  or  $\text{D}_2\text{O}^+$ . The detection of the isotopically scrambled product provides data on the unimolecular decay channel, whereas the observation of  $\text{H}_2\text{O}^+$  or  $\text{D}_2\text{O}^+$  products can be attributed to either charge transfer or unimolecular decomposition; products arising from dissociative processes should be observed near the center of mass of the collision system, while charge transfer products should appear near the direction of the secondary (neutral) beam because such products generally acquire little momentum transverse to the direction of the precursor neutral during electron transfer.<sup>28</sup>

Laboratory angular distributions for the production of  $\text{H}_2\text{O}^+$  in collisions of  $\text{D}_2^+$  with  $\text{H}_2\text{O}$  are shown in Figure 6 at four energies between 1.1 and 6.3 eV. At the lowest collision energy, the distribution shows a strong peak near  $90^\circ$  in the lab, with a slight hint of additional product formation near the center of mass of the system, indicated by an arrow.  $\text{H}_2\text{O}^+$  formed by exothermic charge transfer is expected to be formed with little momentum transfer accompanying electron transfer, generating the peak near  $90^\circ$  in the lab. As the collision energy increases, the "bump" near the centroid becomes more pronounced, although a sharp bump is no longer present at the highest kinetic energy. Although the absolute intensity of the ballistic  $\text{H}_2\text{O}^+$  bump continues to increase at 6.3 eV, its magnitude relative to the intense charge transfer peak at  $90^\circ$  has decreased. Clearly, the enhanced intensity near the centroid must arise from unimolecular decay of the  $\text{DH}_2\text{O}^+$  formed by the initial deuteron transfer to  $\text{H}_2\text{O}$ . We

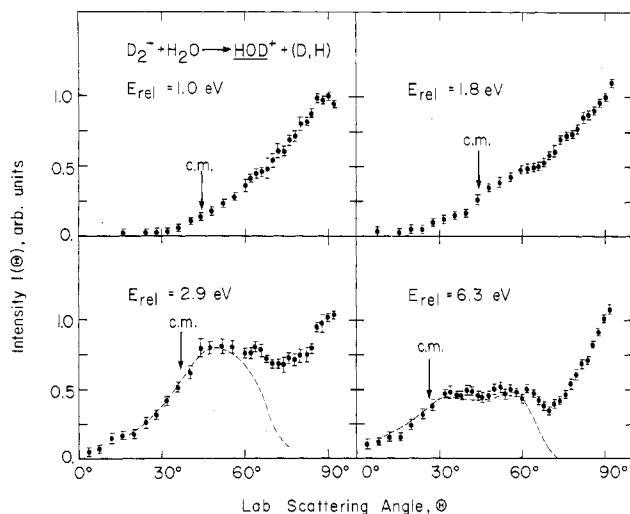


**Figure 7.** Laboratory angular distributions for  $\text{HOD}^+$  produced in collisions of  $\text{D}_2^+$  with  $\text{H}_2\text{O}$  at collision energies indicated. Dotted lines at 2.9 and 6.3 eV are fits resulting from deconvolution of energy scans of  $\text{HOD}^+$  produced by unimolecular decay of  $\text{DH}_2\text{O}^+$ .

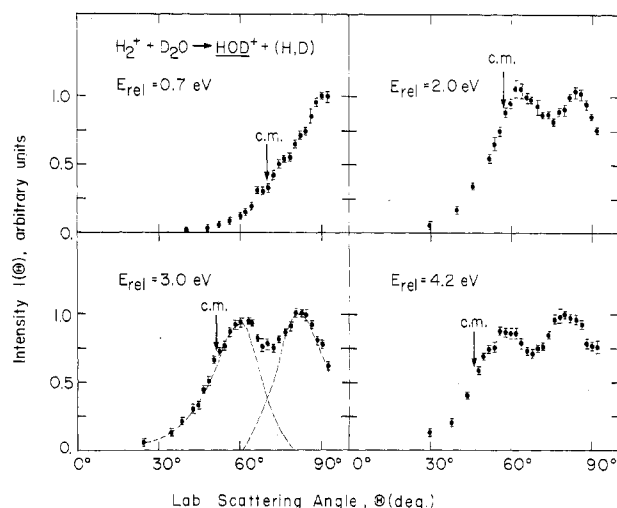


**Figure 8.** Laboratory angular distributions for  $\text{HOD}^+$  produced in collisions of  $\text{H}_2^+$  with  $\text{D}_2\text{O}$  at collision energies indicated. Dotted line peaking near  $60^\circ$  in the 3.0-eV experiment is the fit resulting from deconvolution of energy scans of  $\text{HOD}^+$  produced by unimolecular decay of  $\text{HD}_2\text{O}^+$ . Dotted line peaking near  $90^\circ$  is result of deconvolution of  $\text{HOD}^+$  energy scans produced by four-center exchange reaction  $\text{H}_2^+(\text{D}_2\text{O}, \text{HD})\text{HOD}^+$ .

note that this peak is displaced away from the centroid toward the  $\text{H}_2\text{O}$  beam direction at  $90^\circ$ ; this displacement arises from the initial momentum of the  $\text{DH}_2\text{O}^+$  precursor prior to ejection of a deuterium atom and will be discussed in greater detail in the following paragraphs.

Competing with deuterium emission from the  $\text{DH}_2\text{O}^+$  complex is hydrogen atom emission to yield the  $\text{HOD}^+$  ion; we have measured laboratory angular distributions for  $\text{HOD}^+$  at the same four energies as for  $\text{H}_2\text{O}^+$  formation and show the resultant data in Figure 7. The appearance of product near the centroid becomes increasingly apparent as the collision energy increases; however, the second peak near  $90^\circ$ , which is ascribed to charge transfer in the  $\text{H}_2\text{O}^+$  production channel, is still present in the  $\text{HOD}^+$  data. Clearly, there exists a second process for  $\text{HOD}^+$  formation in addition to unimolecular decay; we comment on the nature of this process later in this section.

The  $\text{HOD}^+$  angular distributions of Figure 7 show that the second channel for  $\text{HOD}^+$  production reaches its peak at or beyond  $92^\circ$  in the laboratory, and therefore out of

(26) M. H. Cheng, M. Chiang, E. A. Gislason, B. H. Mahan, C. W. Tsao, and A. S. Werner, *J. Chem. Phys.*, **52**, 5518 (1970).

(27) B. H. Mahan and P. J. Schubart, *J. Chem. Phys.*, **66**, 3155 (1977).

(28) R. Marx in "Kinetics of Ion-Molecule Reactions", P. Ausloos, Ed., Plenum Press, New York, 1979, p 103.

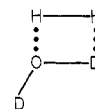
the range of our detector. In order to provide more favorable kinematics for direct observation of the two distinct channels for isotopic exchange, i.e., the channels near the centroid and near the neutral beam direction, we have performed the experiment  $\text{H}_2^+(\text{D}_2\text{O}, \text{HD})\text{HOD}^+$  at four collision energies and show angular distributions for  $\text{HOD}^+$  formation in Figure 8. At the lowest collision energy of 0.7 eV, near threshold for unimolecular decay of  $\text{HD}_2\text{O}^+$ , a single peak appears in the angular distribution near  $90^\circ$ . As the collision energy increases to 2.1 eV, this peak moves away from the direction of the neutral beam to smaller angles, and the second channel, corresponding to unimolecular decay of  $\text{HD}_2\text{O}^+$ , begins to appear near the centroid of the system. The  $\text{H}_2^+ + \text{D}_2\text{O}$  system exhibits favorable kinematics which allow complete resolution of the two channels for isotope scrambling and an essentially complete set of lab fluxes for both channels, thereby allowing for extraction of a reliable cross section over all of barycentric space. The appearance of a product intensity maximum at angles away from the neutral beam also eliminates the concern that the  $\text{HOD}^+$  product near the beam is a background reaction contaminant rather than true product. Furthermore, the cross section for this channel increases with decreasing relative energy, indicative of an exothermic reaction. This result contrasts with the observations of Kim and Huntress,<sup>12</sup> who concluded from ICR line shapes that the  $\text{HOD}^+$  channel increases in cross section with increasing energy. The usual source of background contamination in beam experiments employing seeded neutral beams arises from charge transfer from the  $\text{H}_2^+$  ion beam to  $\text{H}_2$  carrier gas in the neutral beam. The resultant thermal  $\text{H}_2^+$  may then undergo a very rapid proton transfer or exchange reaction with the neutral species; the cross section for  $\text{H}_2^+$  formation by charge transfer increases with ion beam energy, thus generating background signals which generally increase with increasing collision energy. Seeding the  $\text{H}_2\text{O}$  in He eliminates this source of background; such seeding yields bimodal angular distributions like those in Figure 8, demonstrating that the reactions are not artifacts.

At our lowest collision energy of 0.7 eV,  $\text{H}_2^+$  reagents must have vibrational excitation in excess of 0.9 eV in order for the  $\text{HD}_2\text{O}^+$  product to have internal excitation sufficient for dissociation to  $\text{HOD}^+$  or  $\text{D}_2\text{O}^+$ . The Franck-Condon distribution indicates that  $\sim 50\%$  of the  $\text{H}_2^+$  ions have this minimum vibrational excitation, i.e., are in  $v \geq 3$ , and the populations of such species decrease monotonically with increasing vibrational excitation. The most probable relative translational energy for  $\text{HOD}^+ + \text{HD}$  products at this collision energy is  $\sim 0.5$  eV. Only 10% of the  $\text{H}_2^+$  reagents have sufficient internal energy to create  $\text{HOD}^+$  with this much translational energy, leaving the  $\text{HOD}^+$  product with essentially no internal excitation. Such an energy distribution is difficult to reconcile with the very highly internally excited  $\text{HOD}^+$  produced near the centroid and suggests that the mechanism for  $\text{HOD}^+$  production near the neutral beam is not that of unimolecular decay. Furthermore, the fact that the  $\text{HOD}^+$  signal near the neutral beam increases with decreasing collision energy indicates quite strongly that the  $\text{HOD}^+$  is the product of an exothermic chemical reaction.

The ICR data of Kim and Huntress<sup>12</sup> further support the hypothesis that  $\text{HOD}^+$  formation proceeds primarily through a direct reaction at low relative energies. At thermal energies, formation of  $\text{HOD}^+$  by unimolecular decay of  $\text{DH}_2\text{O}^+$  requires a minimum  $\text{D}_2^+$  vibrational excitation of 1.6 eV; only 8% of the  $\text{D}_2^+$  reagents have this minimum vibrational excitation. The fact that the  $\text{HOD}^+$

channel proceeds with a rate 40% as large as the deuteron transfer reaction suggests that the channel must be exothermic. It seems quite unlikely that the cross section for  $\text{HOD}^+$  formation by unimolecular decay of  $\text{DH}_2\text{O}^+$  could be sufficiently large that 8% of the  $\text{D}_2^+$  reagent ions could react to give  $\text{HOD}^+$  at a rate 40% as large as the formation of  $\text{DH}_2\text{O}^+$ , for which deuteron transfer is exothermic for all vibrational states of  $\text{D}_2^+$ .

The appearance of two distinct routes for isotope exchange, one of which involves unimolecular decay of isotopically substituted  $\text{H}_2\text{O}^+$  and shows definite threshold behavior, the second of which is distinct from the products of unimolecular decay observed near the centroid, is quite interesting. In the case of the endothermic unimolecular decay channel, the reaction products must be  $\text{HOD}^+ + \text{H} + \text{D}$ , whereas the most likely exothermic process occurring at lower collision energies should yield  $\text{HOD}^+ + \text{HD}$ , a process releasing 2.8 eV. The observation of  $\text{HOD}^+$  distinct from unimolecular decay suggests very strongly that isotope scrambling occurs by a direct reaction through a transient species involving strong interaction of all five atoms. It is tempting to ascribe the formation of  $\text{HOD}^+$  through this direct reaction to a four-center exchange reaction<sup>29-32</sup> involving the critical configuration



followed by cleavage of the H-H and O-D bonds to give  $\text{DOH}^+ + \text{HD}$  products. The formation of the charge-exchanged products  $\text{HD}^+ + \text{HOD}$  is essentially a thermo-neutral process and is thus less favored statistically than the observed products. Furthermore, the detection of the light ( $\text{HD}^+$ ) product of the chemical reaction is kinematically unfavorable; a detailed search for  $\text{HD}^+$  in these experiments was unsuccessful.

Further data on the dynamics of these reactions may be obtained by measuring their product translational energy distributions. Unfavorable kinematics in the  $\text{D}_2^+ + \text{H}_2\text{O}$  system allow only a determination of product energy distributions for  $\text{HOD}^+$  and  $\text{H}_2\text{O}^+$  produced near the centroid because the channel peaking near  $90^\circ$  in the lab cannot be observed in its entirety. We present differential cross sections for  $\text{H}_2\text{O}^+$  and  $\text{HOD}^+$  production from  $\text{D}_2^+ + \text{H}_2\text{O}$  at a relative energy of 2.9 eV and corresponding data for  $\text{HOD}^+$  production at a relative energy of 6.3 eV.  $\text{H}_2\text{O}^+$  production near the centroid at the higher collision energy is not well resolved from the charge transfer, making a reliable analysis difficult.

In the case of  $\text{H}_2^+ + \text{D}_2\text{O}$  collisions, the production of  $\text{HOD}^+$  by unimolecular decay and four-center exchange is well separated in the laboratory coordinate system, and a fairly complete picture of the differential cross section can be extracted from the data for all collision energies greater than or equal to 2.0 eV. We have measured differential cross sections for these two channels at a collision energy of 3.0 eV. The four-center reaction yielding  $\text{HOD}^+$  may be analyzed in a straightforward way since  $\text{HOD}^+$  is one of two products of a bimolecular reaction; thus the kinematics of the reaction are unique. However, the unimolecular decay channel formally involves the production of three particles,  $\text{HOD}^+ + \text{H} + \text{D}$ , and thus the

(29) S. H. Bauer and E. Ossa, *J. Chem. Phys.*, **45**, 434 (1966).

(30) S. B. Jaffe and J. B. Anderson, *J. Chem. Phys.*, **51**, 1057 (1969).

(31) S. H. Bauer, D. M. Lederman, E. L. Resler, Jr., and E. R. Fisher, *J. Chem. Kinet.*, **5**, 93 (1973).

(32) A. Lifshitz and M. Frenklach, *J. Chem. Phys.*, **67**, 2803 (1977), and references therein.

determination of the momentum of the  $\text{HOD}^+$  product only is insufficient to determine the momenta of all three particles. In the case of  $\text{D}_2^+$  collisions with  $\text{H}_2\text{O}$  and  $\text{H}_2^+$  collisions with  $\text{D}_2\text{O}$ , the initial products,  $\text{DH}_2\text{O}^+$  and  $\text{HD}_2\text{O}^+$ , respectively, acquire momentum, and thus kinetic energy, before their decomposition by H or D atom elimination. Thus, the center of mass for the unimolecular decomposition of  $\text{HD}_2\text{O}^+$  or  $\text{DH}_2\text{O}^+$  is not the center of mass for the original collision creating the decomposing species. Since the momentum of the D (H) atom accompanying  $\text{DH}_2\text{O}^+$  ( $\text{HD}_2\text{O}^+$ ) formation is not determined in these experiments, the initial momentum of the decomposing ion is not known, and the location of the center of mass for the ensuing unimolecular decomposition is also not known precisely. However, the initial proton (deuteron) transfer reaction producing stable  $\text{HD}_2\text{O}^+$  ( $\text{DH}_2\text{O}^+$ ) has an angular distribution which is exceedingly sharp, indicating that the momentum imparted to nascent products is directed essentially exclusively along the initial relative velocity vector. The proton transfer experiments performed at the lowest collision energy where unimolecular decay should be a minor channel suggest that a very small fraction of the total energy available ( $\leq 10\%$ ) appears in product translation; at  $E_{\text{rel}} = 0.7$  eV, the most probable value of  $f_{\text{T}}$  is  $\sim 0.07$ , with the average value of the  $P(f_{\text{T}})$  distribution equal to 0.18. Thus, it is reasonable to model the initial momentum imparted to the  $\text{HD}_2\text{O}^+$  ( $\text{DH}_2\text{O}^+$ ) product as being directed along  $\mathbf{V}_{\text{rel}}$ , corresponding to a small fraction ( $\sim 10\%$ ) of the available energy in translation of nascent  $\text{HD}_2\text{O}^+$  or  $\text{DH}_2\text{O}^+$ . This approach to the unimolecular decay of  $\text{HD}_2\text{O}^+$  and  $\text{DH}_2\text{O}^+$  is quite similar to the "stripping plus dissociation" model applied by Mahan and Schubart<sup>27</sup> to  $\text{DCO}^+$  formation from decomposition of  $\text{DCO}_2^+$  produced in the reaction  $\text{CO}_2^+ + \text{D}_2 \rightarrow \text{DCO}_2^+ + \text{D}$ . In that model, they hypothesized that the nascent  $\text{DCO}_2^+$  product is formed by spectator stripping<sup>19,20</sup> and then decays unimolecularly. Their contour map for  $\text{DCO}^+$  formation from  $\text{DCO}_2^+$  produced at 10.4 eV shows striking symmetry with respect to the spectator stripping velocity.

By assigning a value to the relative translational energy of the products  $\text{DH}_2\text{O}^+ + \text{D}$  or  $\text{HD}_2\text{O}^+ + \text{H}$ , we can compute the initial barycentric speed of  $\text{DH}_2\text{O}^+$  or  $\text{HD}_2\text{O}^+$  prior to dissociation. The spectator stripping model allows us to predict the relative energy of the nascent products, which we denote as  $E_{\text{DH}_2\text{O}^+}$  or  $E_{\text{HD}_2\text{O}^+}$ . The model predicts that  $E_{\text{DH}_2\text{O}^+}$  for the reaction  $\text{D}_2^+ + \text{H}_2\text{O} \rightarrow \text{DH}_2\text{O}^+ + \text{D}$  is 1.3 eV, for an initial relative energy of 2.9 eV, while at 6.3 eV,  $E_{\text{DH}_2\text{O}^+} = 2.8$  eV. In contrast,  $E_{\text{DH}_2\text{O}^+}$  values between 0.25 and 0.50 eV at a relative energy of 2.9 eV, and values between 1.0 and 1.5 eV at a relative energy of 6.3 eV, recover product flux distributions from our data which show symmetry with respect to the centroid defined by the nascent  $\text{DH}_2\text{O}^+$  species. These values of  $E_{\text{DH}_2\text{O}^+}$  and  $E_{\text{HD}_2\text{O}^+}$  provide a better representation of the momentum of the nascent product than does spectator stripping. It appears that the decomposing species is created by a mechanism which imparts it less translational energy than spectator stripping; attractive chemical forces in the exit channel, ignored by the spectator model, may account for this difference. Such an explanation is consistent with the results of Cheng et al.<sup>26</sup> on collision-induced dissociation of molecular ions, in which a strippinglike model accounted for the observed energy distributions of the fragments.

Figure 9 illustrates the kinematic relations involved for the case of  $\text{H}_2^+ + \text{D}_2\text{O}$  yielding  $\text{HD}_2\text{O}^+$ , which then decomposes to  $\text{HOD}^+ + \text{D}$ . The initial barycentric speed imparted to  $\text{HD}_2\text{O}^+$ ,  $\mathbf{u}'_{\text{HD}_2\text{O}^+}$ , is directed along  $\mathbf{V}_{\text{rel}}$ , and the

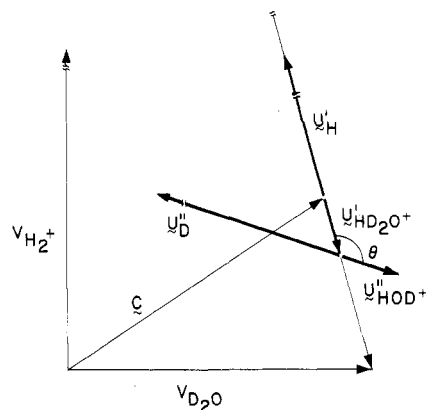


**Figure 9.** Newton diagram illustrating kinematic relations for unimolecular decay of  $\text{HD}_2\text{O}^+$  produced by  $\text{H}_2^+(\text{D}_2\text{O},\text{H})\text{HD}_2\text{O}^+$ .  $\mathbf{u}'_{\text{H}}$  is cm speed of H atom produced by initial formation of  $\text{HD}_2\text{O}^+$ .  $\mathbf{u}'_{\text{D}}$  and  $\mathbf{u}'_{\text{HOD}^+}$  are cm speeds of the fragments of unimolecular decay of  $\text{HD}_2\text{O}^+$ .  $\mathbf{C}$  denotes centroid vector for original  $\text{HD}_2\text{O}^+$  formation, while  $\theta$  is the cm scattering angle for fragmentation relative to the centroid of the decomposing particle.

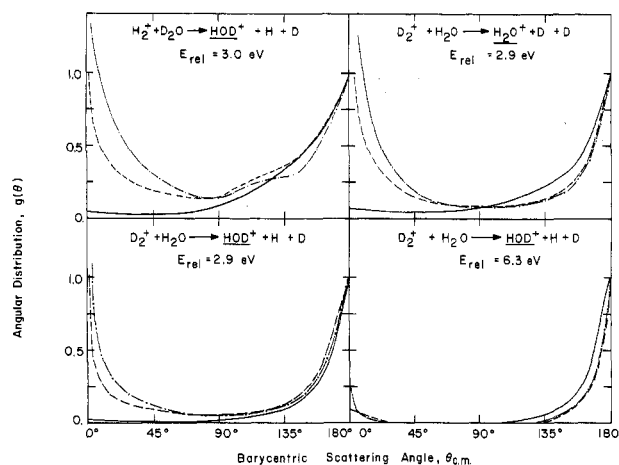


**Figure 10.** Barycentric angular distributions for assumed values of the relative energy of nascent ion prior to decomposition. Upper left:  $E_{\text{HD}_2\text{O}^+} = 0.0$  (—), 0.3 (---), and 0.6 eV (---). Upper right:  $E_{\text{DH}_2\text{O}^+} = 0.0$  (—), 0.25 (---), and 0.50 eV (---). Lower left:  $E_{\text{DH}_2\text{O}^+} = 0.0$  (—), 0.25 (---), and 0.50 eV (---). Lower right:  $E_{\text{DH}_2\text{O}^+} = 0.0$  (—), 1.0 (---), and 1.5 eV (---).

tip of that  $\mathbf{u}$  vector defines the new centroid. The shifting of the centroid toward the neutral ( $\text{D}_2\text{O}$ ) beam explains the appearance of the "bumps" in the angular distributions at laboratory angles larger than the centroid angle of the original collision system. The  $\text{HD}_2\text{O}^+$  product then decomposes, generating the barycentric vectors  $\mathbf{u}'_{\text{HOD}^+}$  and  $\mathbf{u}'_{\text{D}}$  for the fragments and defining the scattering angle  $\theta$ ; since neither  $\mathbf{u}'_{\text{D}}$  nor  $\mathbf{u}'_{\text{H}}$  is measured,  $\mathbf{u}'_{\text{HD}_2\text{O}^+}$  must be treated as a parameter in the kinematic analysis of the unimolecular decay data.

The experimental data for  $\text{H}_2\text{O}^+$  and  $\text{HOD}^+$  production in collisions of  $\text{D}_2^+$  with  $\text{H}_2\text{O}$  and  $\text{HOD}^+$  production from collisions of  $\text{H}_2^+$  with  $\text{D}_2\text{O}$  have been deconvoluted to obtain energy and angular distributions of unimolecular decay products. Four experiments were performed, yielding barycentric angular distributions shown in Figure 10 along with their corresponding energy distributions in Figure 11. Specific values of  $\mathbf{u}'_{\text{HD}_2\text{O}^+}$  or  $\mathbf{u}'_{\text{DH}_2\text{O}^+}$  were assigned to show the sensitivity of the barycentric distributions to the magnitude of the centroid shift; the kinetic energies of  $\text{HD}_2\text{O}^+$  or  $\text{DH}_2\text{O}^+$  were chosen according to the previously mentioned criterion that at low energy the most probable product translational energies are typically  $\leq 10\%$  of the available energy.

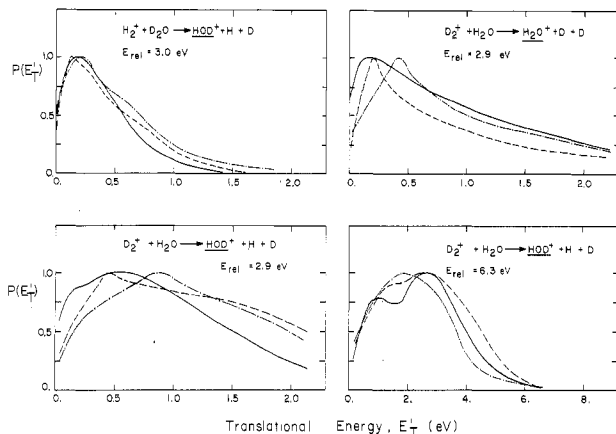


**Figure 11.** Product translational energy distributions for assumed values of the relative energy of the nascent ion prior to decomposition. Legend is the same as for Figure 10. Note change in energy scale for distributions at  $E_{\text{rel}} = 6.3$  eV.

The  $\text{H}_2^+ + \text{D}_2\text{O}$  system at a collision energy of 3.0 eV ( $\bar{E}_{\text{total}} = 8.6$  eV) provides data of excellent quality and yields some very interesting results. When values for the  $\text{HD}_2\text{O}^+$  kinetic energy of 0.3 and 0.6 eV are used, the angular distributions for  $\text{HOD}^+$  formation, shown in the upper left panel of Figure 10, exhibit the striking forward-backward symmetry of a long-lived  $\text{HD}_2\text{O}^+$  complex. The  $1/\sin \theta$  form for the angular distributions is reminiscent of the angular dependence of decay of a prolate symmetric top whose rotational angular momentum is disposed of as product orbital angular momentum.<sup>33</sup> The shape of the angular distribution is relatively insensitive to the initial kinetic energy of nascent  $\text{HD}_2\text{O}^+$ . The product angular distribution for  $E_{\text{HD}_2\text{O}^+} = 0$  is also shown, indicating the apparent backward peaking (with respect to  $\text{H}_2^+$ ) of the  $\text{HOD}^+$  product. The limit as  $E_{\text{HD}_2\text{O}^+}$  approaches zero is quite unrealistic, however, as one certainly expects the nascent  $\text{HD}_2\text{O}^+$  product to carry away a small fraction of the total energy in the proton transfer reaction as translation prior to its decomposition.

The  $\text{HOD}^+$  recoil distributions, shown in the upper left panel of Figure 11, peak at  $\sim 0.15$ – $0.20$  eV, and the shapes of the distributions are quite insensitive to the choice for  $E_{\text{HD}_2\text{O}^+}$ . The recoil distributions are also well-behaved at large translational energies, approaching zero quite smoothly. By assuming only fixed values for  $E_{\text{HD}_2\text{O}^+}$  rather than a distribution as one expects in reactive scattering, one must consider the observed energy and angular distributions extracted from the kinematic analysis only approximate representations. However, the fact that only very small values of  $E_{\text{HD}_2\text{O}^+}$  yield product angular and energy distributions which bear a strong resemblance to those observed in other studies of unimolecular decay suggests that the kinematic analysis presented here is realistic despite the lack of precise knowledge of  $E_{\text{HD}_2\text{O}^+}$ . We will discuss the dynamics of unimolecular decay in greater detail in the next section.

The  $\text{D}_2^+ + \text{H}_2\text{O}$  system at a relative energy of 2.9 eV, although yielding data of lower quality than the previous system, is interesting because of the observation of  $\text{H}_2\text{O}^+$  and  $\text{HOD}^+$ , competitive products of the decomposition of  $\text{DH}_2\text{O}^+$ . Using values of  $E_{\text{DH}_2\text{O}^+} = 0.25$  and 0.50 eV, we have extracted barycentric energy and angular distributions for both decay channels. The angular distributions for both channels show the forward-backward  $1/\sin \theta$  form

factor noted in the previous system, again providing strong evidence for a long-lived complex decaying by transforming its angular momentum to product orbital angular momentum  $L'$ .<sup>34</sup> Although only an approximate model, the elastic spectator model<sup>20</sup> predicts the partitioning of total angular momentum according to the skew angle of the  $\text{H}_2^+ + \text{D}_2\text{O}$  or  $\text{D}_2^+ + \text{H}_2\text{O}$  potential surface and suggests that  $\sim 55\%$  of the initial orbital angular momentum of the reagents should appear as  $\text{HD}_2\text{O}^+$  or  $\text{DH}_2\text{O}^+$  product rotational excitation. When a typical entrance channel impact parameter of 1.0 Å is used, the initial orbital angular momentum of the  $\text{H}_2^+ + \text{D}_2\text{O}$  pair at a relative energy of 3.0 eV is estimated to be  $50\hbar$ ; thus we expect the decomposing  $\text{HD}_2\text{O}^+$  complex to have  $\sim 30\hbar$  of total angular momentum. Since the  $\text{DH}_2\text{O}^+$  or  $\text{HD}_2\text{O}^+$  product is not prolate, the observation of barycentric angular distributions with strong forward-backward peaking suggests that the products of the initial proton or deuteron transfer reaction and their subsequent fragmentation products are formed in the plane defined by the initial reagents. Similar arguments have been made by Becker et al.<sup>35</sup> in their study of  $\text{Li} + \text{HF}$  and  $\text{HCl}$  where strong forward-backward peaking of the products suggests a dynamical planar scattering mechanism in which the potential energy surface exerts a force keeping the three particles in a plane throughout the collision. In the case of decomposition of  $\text{DH}_2\text{O}^+$  or  $\text{HD}_2\text{O}^+$ , the departure of a D or H atom along a line passing through the oxygen atom will yield a fragment with low rotational excitation, thus partitioning the rotational angular momentum of the complex preferentially into product orbital angular momentum. If the decomposing molecule has pyramidal symmetry ( $C_{3v}$ ) rather than planar ( $D_{3h}$ ) symmetry, the departure of D or H should impart some rotational excitation to the molecular ion fragment. A consideration of angular momentum disposal in prolate complexes indicates that the observed angular distribution intensity ratio  $g(\pi)/g(\pi/2)$  between 7 and 10 is consistent with 80–90% of the complex rotational angular momentum appearing in product orbital angular momentum.<sup>34</sup> Thus, molecular ion fragment rotational excitation of up to  $9\hbar$  is consistent with the observed product angular distributions.

The notion that the potential energy surface constrains the reacting particles to a plane is consistent with the suggestion that simultaneous charge transfer-atom transfer may proceed through a four-center critical configuration. It seems plausible to suggest that the same forces in the entrance channel which partition angular momentum of the complex into product orbital angular momentum are operative in facilitating four-center exchange. Theoretical calculations of the surfaces involved in this system would be most helpful in testing this suggestion.

The recoil energy distributions for the  $\text{H}_2\text{O}^+$  product seem fairly well-behaved, although asymptotic approach to zero at large  $E_T'$  is somewhat slow. The recoil distributions of  $\text{HOD}^+$  are less well-behaved, demonstrating poor convergence to zero as  $E_T'$  becomes large. The difficulty of separating  $\text{HOD}^+$  formed by unimolecular decay of  $\text{DH}_2\text{O}^+$  from that formed by the four-center exchange reaction, as well as the severe approximation of assigning a single value to  $E_{\text{DH}_2\text{O}^+}$ , contributes to this behavior. These same problems contribute to the difficulty of assigning an accurate branching ratio to the formation of

(33) W. B. Miller, S. A. Safran, and D. R. Herschbach, *Faraday Discuss. Chem. Soc.*, **44**, 108 (1967).

(34) We note that a long-lived complex may not necessarily yield an angular distribution with forward-backward symmetry. A recent discussion of this may be found in G. M. McClelland and D. R. Herschbach, *J. Phys. Chem.*, **83**, 1445 (1979).

(35) C. H. Becker, P. Casavecchia, P. W. Tiedemann, J. J. Valentini, and Y. T. Lee, *J. Chem. Phys.*, **73**, 2833 (1980).

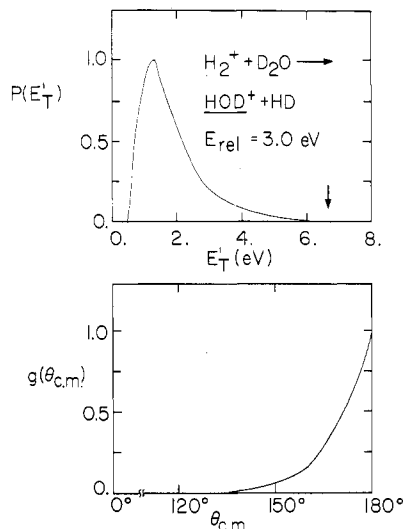


**Figure 12.** Upper panel: Barycentric recoil energy distribution for four-center reaction. Arrow denotes thermochemical limit. Lower panel: Barycentric angular distribution.

$H_2O^+$  and  $HOD^+$  from the same  $DH_2O^+$  precursor, although a very rough value of  $\sigma_{HOD^+}/\sigma_{H_2O^+} \approx 0.7 \pm 0.4$  can be extracted from the data.

At the highest collision energy of 6.3 eV, the  $HOD^+$  product forms a very broad "bump" in the angular distribution of Figure 7; energy distributions measured on  $HOD^+$  product in this ballistic "bump" yield barycentric angular distributions shown in the lower right panel of Figure 10, with  $E_{DH_2O^+}$  chosen to be 1.0 and 1.5 eV. Of special interest is the fact that the forward and backward peaks are now of unequal heights. We note parenthetically that no reasonable value of  $E_{DH_2O^+}$  (up to 3.0 eV) could produce an angular distribution which showed a forward-backward ratio of greater than 0.3. The inequality of the forward and backward peaks at higher collision energies suggests very strongly that the lifetime of the  $DH_2O^+$  species has become comparable to the rotational period; i.e., the complex "osculates" before decomposition.<sup>36-39</sup>

The product recoil distributions at a collision energy of 6.3 eV are shown in the lower right panel of Figure 11 for three values of  $E_{DH_2O^+}$  of 0, 1.0, and 1.5 eV. The recoil distributions are rather broad with their maxima occurring at  $E_T'$  values which correspond to a sizeable fraction of the total available energy in product translation. This behavior of the energy distribution, in conjunction with the apparent "osculatory" behavior evidenced in the product angular distributions, will be very important in assessing intramolecular energy transfer in the  $DH_2O^+$  product prior to its decomposition.

Integration of the deconvoluted (calculated) laboratory fluxes over laboratory velocity to yield angular distributions for comparison with the appropriate data of Figures 6-8 was performed for the four experiments where unimolecular decay products were studied. The angular distribution data of Figure 6-8 show smooth curves through these calculated points, illustrating the quality of the fit to the data as well as the manner in which the unimolecular decay channel was separated from the direct exchange process.

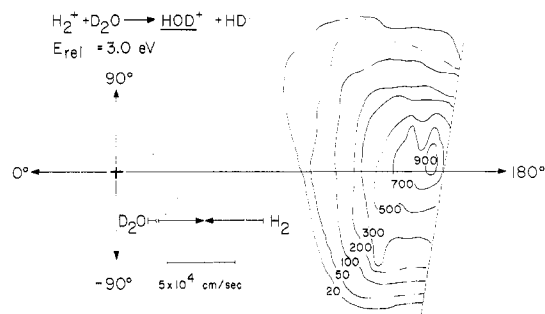


**Figure 13.** Barycentric polar flux contour map for four-center exchange reaction at 3.0 eV.

The experimental angular distributions for  $HOD^+$  formation from  $H_2^+ + D_2O$ , shown in Figure 8, indicate that the favorable kinematics allow most of the  $HOD^+$  intensity arising from the four-center exchange reaction to be observable within the angular range of the apparatus. Accordingly, full energy and angular distribution data were obtained at a relative collision energy of 3.0 eV. These data have been deconvoluted to yield barycentric energy and angular distributions. The smooth curve drawn through the integrated lab fluxes shown in Figure 8 illustrates the separation of the two routes for  $DOH^+$  formation. The energy and angular distributions for this direct reaction are shown in Figure 12; the angular distribution is quite sharply peaked at  $180^\circ$  with respect to the incoming  $H_2^+$  projectile, indicating that the cleavage of the H-H and O-D bonds releases very little momentum transverse to the relative velocity vector. The recoil energy distribution shows a very sharp peak at low  $E_T'$  which falls very rapidly to zero on the low-energy side. The apparent lack of product below 0.5 eV arises from the dissociation channels for the products, the dissociation of  $HOD^+$  to  $OH^+$  ( $OD^+$ ) and D ( $H$ ) occurring at 5.7 eV and dissociation to  $OH$  ( $OD$ ) and  $D^+$  ( $H^+$ ) at 6.1 eV.<sup>17</sup> Figure 13 shows a contour polar flux map for  $HOD^+$  production from the four-center reaction which underscores the essentially direct nature of the isotopic exchange reaction.

In their discussion on the production of  $DCO^+$  in the reaction  $CO_2^+ + D_2 \rightarrow DCO^+ + OD$ , Mahan and Schubart<sup>27</sup> suggested that a direct reaction in which the CO fragment in  $CO_2^+$  interacts only with one deuterium atom in  $D_2$ , the other D atom interacting only with the remaining O atom in  $CO_2^+$ , might account for the formation of  $DCO^+$  at high collision energy. Such a "double stripping" mechanism, applied to  $H_2^+ + D_2O \rightarrow HOD^+ + H_2$ , in which the OD-H and H-D momenta are conserved separately predicts that the product translational energy at a relative kinetic energy of 3.0 eV should be 0.3 eV.  $HOD^+$  products with so little translation should dissociate to  $OD^+$  and  $OH^+$ . The observed most probable translational energy of  $\sim 1.3$  eV reflects the fact that the more highly vibrationally excited states of  $HOD^+$  have undergone dissociation. The prediction of the double stripping model, while quantitatively invalid because of dissociation, is qualitatively correct in predicting the backward scattering behavior of  $HOD^+$  as well as the formation of products with very high internal excitation.

Favorable kinematics and energetics allow us to distinguish between  $HOD^+$  produced by unimolecular decay and four-center (double stripping) exchange. This contrasts with the  $CO_2^+ + D_2$  system in which  $DCO^+$  formation was suggested to occur by both routes, but less favorable kinematics prevented a separation of the two routes. The present system is particularly interesting because the separation of the two channels provides detailed insight

(36) J. D. McDonald, Ph.D. Dissertation, Harvard University, Cambridge, MA, 1971.

(37) S. Stolte, A. E. Proctor, and R. B. Bernstein, *J. Chem. Phys.*, **61**, 3855 (1974).

(38) J. M. Farrar and Y. T. Lee, *J. Chem. Phys.*, **63**, 3639 (1975).

(39) Z. Herman, A. Lee, and R. Wolfgang, *J. Chem. Phys.*, **51**, 452 (1969).

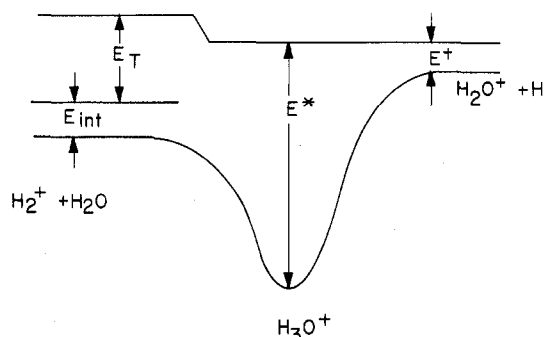


**Figure 14.** Schematic reaction coordinate for  $\text{H}_2^+(\text{H}_2\text{O,H})\text{H}_3\text{O}^+$  and subsequent decay of  $\text{H}_3\text{O}^+$  (and isotopic variants). Break in total energy available to  $\text{H}_3\text{O}^+$  as internal energy in the activated ion,  $E^*$ , arises from energy removed from products as relative translational energy of  $\text{H}_3\text{O}^+$  and H.

into the dynamics of the exchange reaction, the nature of unimolecular production of  $\text{HOD}^+$ , and details of the dynamics of the initial proton transfer yielding nascent  $\text{HD}_2\text{O}^+$ .

### Discussion

The foregoing data analysis has demonstrated that the proton transfer reaction to  $\text{H}_2\text{O}$  forming  $\text{H}_3\text{O}^+$  or an isotopically labeled variant is a direct, impulsive reaction over the entire range of collision energies studied. The substantial exothermicity of the proton transfer in reaction 1 makes unimolecular decay of the hydronium ion an important channel for reaction over the entire collision energy range of these experiments. The translational energy spectra of the products, shown in Figure 5, indicate that the products tend to maximize their internal excitation subject to product stability considerations. Because the onset of dissociation occurs at very low translational energy, the common mechanisms for direct, impulsive reactions, specifically the spectator stripping model,<sup>19,20</sup> are invalid. Despite the fact that we are unable to observe a sizeable fraction of the nascent products of the proton transfer reaction because of dissociation, the direct observation of the products of unimolecular decay allows us to draw conclusions about the formation of the precursor ion.

A schematic reaction coordinate which illustrates pictorially the energetics of unimolecular decay is shown in Figure 14. The lifetime of the  $\text{H}_3\text{O}^+$  complex can be estimated from RRKM theory.<sup>40,41</sup> At low collision energies particularly, the lifetime of  $\text{H}_3\text{O}^+$  should be sufficiently long to allow the ion to live several rotational periods, enough to ensure for the vast majority of realistic cases<sup>34</sup> a barycentric angular distribution symmetric about  $\theta = \pi/2$ . At a relative energy of 3.0 eV, an  $\text{H}_3\text{O}^+$  complex should have a lifetime which ranges between 2 and 40 ps. Such a long lifetime justifies our procedure for estimating the initial barycentric speed of nascent  $\text{HD}_2\text{O}^+$  or  $\text{DH}_2\text{O}^+$  products prior to their observed decomposition.

The barycentric angular distributions of Figure 10 for the formation of  $\text{HOD}^+$  and  $\text{H}_2\text{O}^+$  from  $\text{DH}_2\text{O}^+$  at translational energies near 3.0 eV show the expected forward-backward symmetry in the decay of a long-lived complex. The reaction coordinate justifies the assumption that the nascent product lives several rotational periods. Because the observation of the momentum of one of three particles produced by unimolecular decay is kinematically insuffi-

cient to define the reaction dynamics uniquely,<sup>26</sup> the assignment of the initial kinetic energy of the nascent product consistent with a symmetric angular distribution for unimolecular decay is a realistic procedure. As indicated in the data analysis, such symmetric distributions are consistent with the production of nascent  $\text{HD}_2\text{O}^+$  or  $\text{DH}_2\text{O}^+$  with substantially less translation than predicted by spectator stripping or the closely related direct interaction with product repulsion (DIPR) model.<sup>42</sup> With most probable translational energies in the range of 5–10% of the total available energy as suggested by our analysis of the unimolecular decay, the dynamics of proton transfer, while appearing to be direct, involve substantial forces as the products separate which reduce the translational energy of the products. Such behavior has also been noted in the direct collision-induced dissociation of molecular ions by a variety of targets.<sup>26</sup>

The barycentric angular distributions for  $\text{HOD}^+$  and  $\text{H}_2\text{O}^+$  emission from  $\text{DH}_2\text{O}^+$  and  $\text{HOD}^+$  emission from  $\text{HD}_2\text{O}^+$  at relative energies near 3.0 eV, shown in Figure 10, indicate strong forward-backward peaking, yielding distributions which strongly resemble  $1/\sin \theta$  distributions. The appearance of such strong forward-backward peaking in the unimolecular decay of  $\text{DH}_2\text{O}^+$  and  $\text{HD}_2\text{O}^+$  cannot be explained by angular momentum conservation constraints alone. In fact, such conservation constraints alone would suggest that a large fraction of the rotational angular momentum of the complex is disposed of as product rotation, rather than as orbital angular momentum. Since the initial angular momentum of  $\text{H}_2^+ + \text{D}_2\text{O}$  or  $\text{D}_2^+ + \text{H}_2\text{O}$  is primarily orbital, the observation of strong forward-backward peaking in the decay of  $\text{HD}_2\text{O}^+$  and  $\text{DH}_2\text{O}^+$  suggests that the rotational angular momentum of the nascent product is strongly polarized parallel to the initial angular momentum. Thus, there must also exist a strong correlation between  $\mathbf{J}'$  and  $\mathbf{L}'$ , the rotational excitation of the nascent complex and its orbital angular momentum relative to the departing H or D atom. Furthermore, the rotational angular momentum of the  $\text{HD}_2\text{O}^+$  or  $\text{DH}_2\text{O}^+$  complex must be disposed of in such a manner as to correlate  $\mathbf{J}''$  and  $\mathbf{L}''$ , the rotational angular momentum of  $\text{HOD}^+$  or  $\text{H}_2\text{O}^+$  and the relative orbital angular momentum of the fragments of  $\text{HD}_2\text{O}^+$  or  $\text{DH}_2\text{O}^+$  decay, respectively. In order to observe the forward-backward peaking,  $\mathbf{J}''$  must be parallel to  $\mathbf{L}''$  in the decomposition step. Herschbach and co-workers have provided experimental<sup>43</sup> and theoretical discussions<sup>34,44,45</sup> of angular momentum polarization in chemical reactions; the elastic spectator stripping mechanism,<sup>20</sup> however, provides a relatively simple model for the initial formation of  $\text{HD}_2\text{O}^+$  and  $\text{DH}_2\text{O}^+$  which predicts angular momentum polarization and the correlation of the rotational excitation of the nascent product with the orbital angular momentum of the initial products. Decomposition of the nascent  $\text{HD}_2\text{O}^+$  or  $\text{DH}_2\text{O}^+$  in a plane perpendicular to its rotational angular momentum vector would then manifest itself as the strong forward-backward peaking observed. The present results appear to confirm the angular momentum polarization predictions of spectator stripping, although the products have more internal excitation than predicted by the model. In this case, forces experienced by the departing products appear to partition the energy into higher internal excitation without destroying the apparent angular momentum polarization.

(43) C. Maltz, N. D. Weinstein, and D. R. Herschbach, *Mol. Phys.*, **24**, 133 (1972).

(44) D. A. Case and D. R. Herschbach, *J. Chem. Phys.*, **64**, 4212 (1976).

(45) D. A. Case, G. M. McClelland, and D. R. Herschbach, *Mol. Phys.*, **35**, 541 (1978).

(40) R. A. Marcus, *J. Chem. Phys.*, **20**, 359 (1952).

(41) P. J. Robinson and K. A. Holbrook, "Unimolecular Reactions", Wiley, New York, 1972.

(42) P. J. Kuntz, *Chem. Phys. Lett.*, **4**, 129 (1969).

While Case and Herschbach<sup>44</sup> have suggested that angular momentum constraints alone tend to make  $J'$  and  $L'$  antiparallel, one must consider the possibility that angular momentum correlations may also convey dynamical information. Hijazi and Polanyi<sup>46</sup> have shown in trajectory studies with three atoms of equal masses that  $L'$  and  $J'$  tend to be antiparallel as products separate on a repulsive surface. The present work suggests that  $L'$  and  $J'$  associated with formation of  $\text{HD}_2\text{O}^+$  or  $\text{DH}_2\text{O}^+$  via a stripping reaction are correlated in a parallel fashion, while  $L''$  and  $J''$  associated with decomposition to  $\text{HOD}^+$  or  $\text{H}_2\text{O}^+$  may be either parallel or antiparallel but are nonetheless highly correlated. Such correlations almost certainly result from a dynamical planar scattering mechanism rather than a simple consequence of angular momentum conservation.

The product translational energy distributions for unimolecular decay, shown in Figure 11, are somewhat dependent on the choice of the initial kinetic energy of the decomposing fragment but, nonetheless, contain important information regarding intramolecular energy transfer in the activated molecule prior to decomposition. The central hypothesis of RRKM theory,<sup>40</sup> that such energy transfer is rapid on the timescale of chemical reactions, has been subjected to a variety of experimental tests in recent years. Since RRKM theory computes rate constants, deducing translational energy distributions from the theory requires several additional hypotheses.<sup>47,48</sup> In particular, if a complex is "tight", i.e., the reverse association has an activation barrier, implying that product rotations correspond to bending vibrations in the complex, exit channel interactions may be substantial, yielding translational energy distributions which are not representative of the energy distribution at the critical configuration.

A variety of refinements to these models for predicting product translational energy distributions have appeared in the literature in recent years.<sup>49-52</sup> Of particular interest is the observation<sup>50</sup> that an incorrect treatment of flux conservation in earlier work<sup>49</sup> underestimates the product translational energy; a more nearly correct treatment yields recoil distributions in closer accord with experiment, but still underestimates product translation in many cases.

The phase space theory of Light and co-workers<sup>53-55</sup> provides a treatment of translational energy distributions less parametric than RRKM by computing the phase space volume accessible to products consistent with energy and angular momentum conservation. Once the criteria for the angular momentum disposal in the decomposition of the complex have been prescribed, the enumeration of the accessible states yields the product recoil distribution. In the present case, we must compute phase space volumes accessible to a  $\text{DH}_2\text{O}^+$  complex as it decomposes by H or D atom emission. The  $\text{DH}_2\text{O}^+$  complex is created with total energy and angular momentum dictated by the dynamics of the original deuteron transfer reaction  $\text{D}_2^+ + \text{H}_2\text{O} \rightarrow \text{DH}_2\text{O}^+ + \text{D}$  rather than by the long-range potential experienced by the approaching reagents. Thus, the total

TABLE I: Phase Space Parameters

parameter	$\text{H}_2\text{O}^+$	$\text{HOD}^+$	parameter	$\text{H}_2\text{O}^+$	$\text{HOD}^+$
$\nu_1$	3223 $\text{cm}^{-1}$	2401 $\text{cm}^{-1}$	$\beta^a$	0.8613	0.8479
$\nu_2$	1408 (2)	1238 (2)	$E_Z$	0.57 eV	0.48 eV
$\nu_3$	3117	2790			

<sup>a</sup> Whitten-Rabinovitch parameters, ref 56.

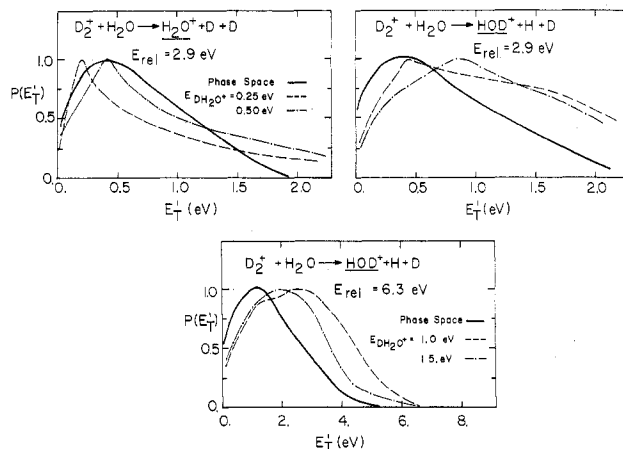


Figure 15. Comparison of observed translational energy distributions and results of phase space calculations for  $\text{H}_2\text{O}^+$  and  $\text{HOD}^+$  formation from  $\text{DH}_2\text{O}^+$  at 2.9 eV and  $\text{HOD}^+$  formation from  $\text{DH}_2\text{O}^+$  at 6.3 eV. Legend is identical for the two experiments at 2.9 eV.

energy and angular momentum of the complex must be regarded as parameters; we have already discussed methods for estimating the total energy. The departing fragments, an atom and a triatomic molecule, experience an  $R^{-4}$  ion-induced dipole potential which determines the maximum allowed product orbital angular momentum through the complex's ability to surmount the exit channel centrifugal barrier:

$$L'_{\max} = 2(E_T')^{1/4}(C_4')^{1/4}(\mu')^{1/2}/\hbar$$

where  $E_T'$  is the final translational energy,  $\mu'$  the product reduced mass, and  $C_4'$  the long-range exit channel force constant.  $C_4'$  is given as  $\alpha e^2/2$ , the polarizability of the hydrogen atom,  $\alpha$ , equal to  $0.666 \text{ \AA}^3$ .<sup>56</sup> Such a model hypothesizes no appreciable exit channel potential barrier to product formation. In the present calculations, we approximate the  $\text{H}_2\text{O}^+$  or  $\text{HOD}^+$  as a symmetric top by averaging together the smallest two rotational constants; thus the formulation of phase space theory given by Parson et al.<sup>57</sup> for a symmetric top plus an atomic product is directly applicable. The Light-Pechukas version of the phase space theory with an  $R^{-4}$  potential should be equivalent to the Klots-Chesnavich-Bowers formulations.<sup>51,52</sup> The vibrational densities of states for  $\text{HOD}^+$  and  $\text{H}_2\text{O}^+$  are given by a semiclassical formula,<sup>58,59</sup> using the  $\text{H}_2\text{O}^+$  bending vibration measured by Lew<sup>60</sup> and scaling the symmetric and antisymmetric stretches of  $\text{H}_2\text{O}$  and  $\text{HOD}^+$  in the ratio of the  $\text{H}_2\text{O}^+$  bending frequency to the

(46) N. H. Hijazi and J. C. Polanyi, *J. Chem. Phys.*, **63**, 2249 (1975); *Chem. Phys.*, **11**, 1 (1975).

(47) R. A. Marcus, *J. Chem. Phys.*, **62**, 1372 (1975).

(48) G. Worry and R. A. Marcus, *J. Chem. Phys.*, **67**, 1636 (1977).

(49) S. A. Saffron, N. D. Weinstein, D. R. Herschbach, and J. C. Tully, *Chem. Phys. Lett.*, **12**, 564 (1972).

(50) L. Holmlid and K. Rynefors, *Chem. Phys.*, **19**, 261 (1977).

(51) C. E. Klots, *J. Chem. Phys.*, **64**, 4269 (1976).

(52) W. J. Chesnavich and M. T. Bowers, *J. Am. Chem. Soc.*, **98**, 8301 (1976); **99**, 1705 (1977).

(53) J. C. Light, *Discuss. Faraday Soc.*, **44**, 14 (1967).

(54) P. Pechukas, J. C. Light, and C. Rankin, *J. Chem. Phys.*, **44**, 794 (1966).

(55) J. Lin and J. C. Light, *J. Chem. Phys.*, **45**, 2545 (1966).

(56) J. O. Hirschfelder, C. F. Curtiss, and R. B. Bird, "Molecular Theory of Gases and Liquids", Wiley, New York, 1954, p 946.

(57) J. M. Parson, K. Shobatake, Y. T. Lee, and S. A. Rice, *J. Chem. Phys.*, **59**, 1402 (1973).

(58) G. Z. Whitten and B. S. Rabinovitch, *J. Chem. Phys.*, **38**, 2466 (1963).

(59) Reference 41, p 136, shows that the Whitten-Rabinovitch approximation should be accurate to within a few percent for molecules with vibrational energy greater than or equal to ca. one-half the zero-point energy of the molecule.

(60) H. Lew, *Can. J. Phys.*, **54**, 2028 (1976).

H<sub>2</sub>O bending frequency. The parameters for the phase space calculation are shown in Table I. Our calculations show that the recoil energy distributions are quite insensitive to the total angular momentum of the complex over a range from  $5\hbar$ – $50\hbar$ .<sup>57</sup> The results of the recoil energy calculations for H<sub>2</sub>O<sup>+</sup> and HOD<sup>+</sup> formation from DH<sub>2</sub>O<sup>+</sup> at a relative energy of 2.9 eV and HOD<sup>+</sup> from DH<sub>2</sub>O<sup>+</sup> at 6.3 eV are shown in Figure 15 for a total angular momentum of  $25\hbar$ .

The calculations demonstrate reasonable agreement with experiment for the two lower energy recoil distributions. Underestimation of high recoil speeds is particularly noticeable in the HOD<sup>+</sup> recoil distributions. In light of the approximate procedure for extracting these distributions, however, it appears reasonable to consider the model consonant with the data.

The model calculation for HOD<sup>+</sup> formation at the higher energy seriously underestimates high translational energy products regardless of the amount of initial kinetic energy assigned to DH<sub>2</sub>O<sup>+</sup>. However, the barycentric angular distribution for HOD<sup>+</sup> formation shown in the lower right panel of Figure 10 indicates that, at this collision energy, the complex "osculates" with a lifetime comparable to a rotational period. The ratio of the forward to backward peaks is  $\sim 0.3$ , corresponding to a lifetime of  $\sim 0.4$  times the rotational period.<sup>62</sup> For a DH<sub>2</sub>O<sup>+</sup> complex with  $25\hbar$  of rotational angular momentum about the A axis, the rotational period is estimated to be  $\sim 2 \times 10^{-15}$  s, significantly less than a vibrational period and certainly too short for rapid redistribution of energy within the complex.

In addition to the fact that the lifetime of the decomposing complex is too short for rapid equilibration of the energy deposited by O–D bond formation, the appearance of rather high product recoil energies is consistent with increased dominance of product orbital angular momentum as the collision energy increases. This effect, noted in previous work on F + CH<sub>3</sub>I<sup>38</sup> and Hg + I<sub>2</sub>,<sup>23</sup> suggests that the rotational angular momentum of the complex couples to product translation with increasing effectiveness as the collision energy increases. This effect is indicative of a substantially elongated O–D or O–H fragmenting bond in the critical configuration.

Although the DH<sub>2</sub>O<sup>+</sup> complex appears to behave fairly statistically at a collision energy of 3.0 eV, as evidenced by the recoil energy distributions, the branching ratio for HOD<sup>+</sup> to H<sub>2</sub>O<sup>+</sup> formation by unimolecular decay, estimated from statistical arguments to be at least 3, is much closer to unity. The appearance of more H<sub>2</sub>O<sup>+</sup> than pre-

dicted statistically would suggest that the complex "remembers" that the O–D bond contains excess energy at the moment DH<sub>2</sub>O<sup>+</sup> is formed, preferentially cleaving that bond upon decay, although such an effect does not manifest itself in the recoil energy distributions.

Of significant interest in this work is the observation of HOD<sup>+</sup> formation in the reaction of H<sub>2</sub><sup>+</sup> with D<sub>2</sub>O without involvement of a decaying HD<sub>2</sub>O<sup>+</sup> product. The thermochemistry and kinematics as described by the double stripping mechanism<sup>27</sup> argue in favor of a four-center exchange reaction. The apparent observation of such reactions has been the subject of much controversy, although the H<sub>2</sub>–D<sub>2</sub> exchange reaction provides some of the strongest evidence in favor of such a mechanism. The electronic orbital correlation rules of Woodward and Hoffmann<sup>63</sup> argue that the four-center reaction is thermally forbidden, a substantial potential energy barrier between reactants and products arises from the fact that the orbitals of the ground-state reagents correlate with an excited state of the intermediate. Such an argument is likely to be more valid in cases of high symmetry, such as the H<sub>2</sub>–D<sub>2</sub> exchange reaction, than in the rather low-symmetry case here. If a symmetry-imposed barrier to four-center exchange is present in this system, it may be several tenths of an eV in magnitude. However, in the studies at hand, the product HOD<sup>+</sup> is observed at collision energies below 1 eV, with H<sub>2</sub><sup>+</sup> reagents which have up to 2.6 eV of internal excitation. The role of reagent internal excitation in promoting the four-center H<sub>2</sub> + D<sub>2</sub> reaction has been emphasized in the laser excitation experiments of Bauer et al.,<sup>31</sup> the interpretation of which is consistent with the present work in which H<sub>2</sub><sup>+</sup> vibrational excitation may be efficacious in surmounting a symmetry-imposed barrier.

In conclusion, the H<sub>2</sub><sup>+</sup> + H<sub>2</sub>O system with isotopic variants presents a substantial challenge to the chemical dynamicist. The observation of the products of unimolecular decay allows one to discuss the dynamics of that process as well as to speculate about the dynamics of proton transfer creating the nascent (unobserved) products which ultimately decompose. The suggestion that the reactive scattering occurs in a single plane with strong angular momentum correlations, combined with the observation of a four-center exchange reaction, indicates that the potential surface has interesting features worthy of theoretical investigation.

*Acknowledgment.* This research has been supported by the U.S. Department of Energy. We acknowledge helpful conversations with Mr. Scott Anderson on the role of highly vibrationally excited H<sub>2</sub><sup>+</sup> reaction dynamics.

(61) G. Herzberg, "Infrared and Raman Spectra", Van Nostrand, New York, 1945, pp 280–2.

(62) G. A. Fisk, J. D. McDonald, and D. R. Herschbach, *Faraday Discuss. Chem. Soc.*, **44**, 228 (1967).

(63) R. B. Woodward and R. Hoffmann, "The Conservation of Orbital Symmetry", Academic Press, New York, 1970.